Optik - International Journal for Light and Electron Optics 244 (2021) 166695

Contents lists available at ScienceDirect

Optik

journal homepage: www.elsevier.com/locate/ijleo

Original research article

Structural and an orange-red emission studies of Sm^{3+} doped $Ba_3La_2(BO_3)_4$ phosphor for solid state lighting application

M. Peddaiah *, C. Salma, B. Hemalatha Rudramadevi

Department of Physics, Sri Venkateswara University, Tirupati, AP, 517502, India

ARTICLE INFO

Keywords:
Emission
Phosphors
Rare earth
Color chromaticity
Solid-state reaction

ABSTRACT

A new kind of host phosphor materials $Ba_3La_2(BO_3)_4$ doped with Sm^{3+} ion, were prepared by solid state reaction method. The crystal structure of synthesized samples is an orthorhombic structure confirmed by XRD study. The FTIR spectra confirmed the band assignments among the borate networks. The thermal stability of the sample was examined by TG-DTA study. FESEM and EDX provide surface morphology and elemental composition of the materials. From DRS analysis we have calculated the energy band gap through Tauc plot method. For PL studies, $Ba_3La_2(BO_3)_4$: Sm^{3+} samples excitation spectra were monitored at 601 nm and the prominent excitation peak was observed at 408 nm. The emission spectra consist of four bands and the highest intense emission peak was observed at 601 nm ($^4G_{5/2} \rightarrow {}^6H_{7/2}$) due to the intra 4f transition of the Sm^{3+} ion. From CIE 1931 Chromaticity, the color coordinates were calculated x = 0.5363; y = 0.4519 and these are lying in the orange-red region. Hence this new phosphor sample might be a useful material for an orange-red emission, applicable in solid-state lighting and display devices.

1. Introduction

Researchers extensively investigating on the present and future generations of white light emission diodes (W-LEDs), field emission displays (FEDs) and plasma display panels (PDPs) that have been occupied by the inorganic phosphor materials which can have superior characteristics of high luminous efficiency, energy saving, chemical stability and eco-friendly [1,2]. W-LEDs based on phosphor materials and have attractive features as solid-state lighting sources since they can have several advantages over fluorescent and incandescent lamps including cheap cost, high efficiency, energy conservation, high compactness, high thermal stability, good reliability and longer operating life [3–5]. Many research groups have been paid efforts to synthesize red emitting phosphor suitable for LEDs [6]. Among the rare earth elements, trivalent samarium ion (Sm^{3+}) usually emits orange-red light when excited with blue and near ultraviolet and commonly has a elevated emission intensity [7,8].

The luminescent characteristics are varying based on the host material and hence host material selection is most important. The selected host materials that have high crystallanity, thermal stability, chemical stability, low phonon energy and superior transparency in an ultra violet [UV] region are best suitable for luminescent materials [9–11]. Borate based oxide materials could show these characteristics and hence many pioneering researchers have worked on borate based phosphor materials. The present $Ba_3La_2(BO_3)_4$ material belongs to borate group inorganic phosphor material which have orthorhombic crystal structure with space group pcmn (62)

* Corresponding author.
E-mail address: midde.peddaiah@gmail.com (M. Peddaiah).

https://doi.org/10.1016/j.ijleo.2021.166695
Received 20 January 2021; Received in revised form 4 March 2021; Accepted 5 March 2021
Available online 30 June 2021

[12]. In addition, the lanthanum ion (La^{3+}) is more suitable for doping with sm^{3+} ion because of both ions are belongs to lanthanide group and have same oxidation state and ionic radius also almost similar. Best our knowledge and according to literature still now no one has reported Ba_3La_2 $(BO_3)_4$: Sm^{3+} phosphor materials.

2. Experimental

2.1. Material preparation

In this present work, the $Ba_3La_2(BO_3)_4$ doped with trivalent samarium (Sm^{3+}) phosphor synthesized by the conventional solid state reaction method using high purity of oxides. The analytical grade of $BaCO_3$ (AR 99.5 %), La_2O_3 (AR 99.9 %), H_3BO_3 (AR 99 %) and Sm_2O_3 (99.9 %) were used as starting materials. A 5-gram batch was prepared by taking exact weight proportions of starting elements according to their molecular weights. The finely powdered mixture was annealed at 900 °C for 5 h, we could obtain Ba_3La_2 $(BO_3)_4$: xSm^{3+} phosphor materials with various concentrations x = 0.02, 0.04, 0.06, 0.08 and 0.1 mol. The chemical equation of the sample is:

$$3BaCO_3+(1\text{-}x)La_2O_3 + xSm_2O_3+ 4H_3BO_3 \rightarrow Ba_3La_{2\ -2x}Sm_{2x}(BO_3)_4 + 6H_2O\uparrow + 3CO_2\uparrow$$

2.2. Materials characterization

The prepared Ba_3La_2 $(BO_3)_4$: xSm^{3+} (x = 0.02, 0.04, 0.06, 0.08 and 0.1 mol) phosphor samples were analyzed through various characterizations techniques. The phase structure and crystalline nature were analyzed by XRD using Bruker D8-Advance diffractometer. FTIR analysis was employed to detect borate-oxygen and metal-oxygen vibrational bands. The thermal stability and heat reactions were examined by TG-DTA using TA instrument, SDT Q600 model. The surface morphology images with different resolutions were recorded by FESEM using TESCAN-MIRA3 analyzer. The starting elements of synthesized phosphor samples were confirmed by using EDX through X-Flash BRUKER analyzer. The photoluminescence studies were carried out by using fluorolog-FL3-11. All the above characterizations were done at room temperature.

3. Results and discussion

3.1. X-ray diffraction studies

The Sm^{3+} doped Ba_3La_2 $(BO_3)_4$ samples were synthesized by solid state reaction method and their phase purity can be confirmed by XRD measurements. The XRD profiles of $Ba_3La_2(BO_3)_4$: xSm^{3+} (x = 0.02, 0.04, 0.06, 0.08 and 0.1 mol) phosphors have shown in the Fig. 1. The doping of Sm^{3+} ion to the host sample was done by the reduction of the exact mol% of La^{3+} ions. It was clear that all the XRD patterns were similar to one another which are the evidence that by the addition of Sm^{3+} ions to the host material, the basic crystal structure does not changed that indicates Sm^{3+} ions can be easily occupied in the vacancies of La^{3+} ions in the crystal lattice. In addition, all the patterns and their phases were in good agreement with the JCPDS card no.77-0546 of Ba_3La_2 $(BO_3)_4$. Hence the crystal structure was confirmed as primitive orthorhombic structure with space group Pcmn (62) with lattice parameters a = 7.734 Å, b=17.043 Å, c=9.056 Å and lattice angles $\alpha = \beta = \gamma = 90°$. The lattice cell volume V = 1193.68 $Å^3$ and its coordination numbers is Z = 4.

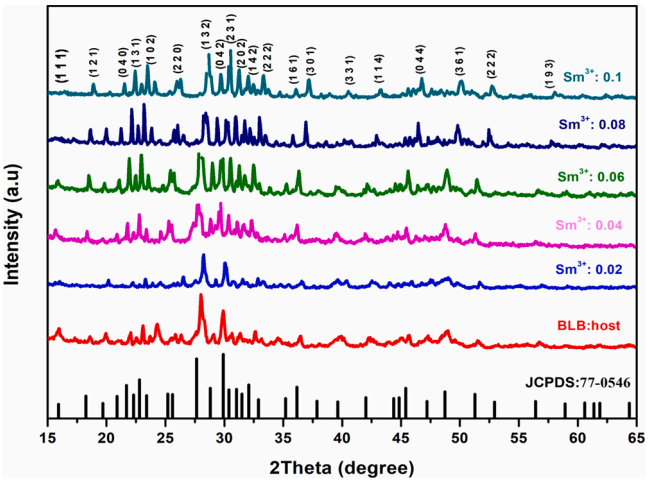

Fig. 1. XRD profiles of Ba_3La_2 $(BO_3)_4$: xSm^{3+} phosphors.

The crystallite size (D) of the phosphor samples have been calculated by using Debye-Scherer's formula [13],

$$D = \frac{0.89\lambda}{\beta Cos\theta} \quad (1)$$

where $\lambda = 0.15406$ nm is the wavelength of the incident x-rays, β is the full width half maxima (FWHM) of strongest diffraction peak and θ be the diffraction angle. The crystallite sizes and dislocation densities of various concentrations of Sm^{3+} doped phosphors were calculated and the details were shown in Table1.

3.2. FTIR analysis

The Fourier Transform Infrared (FTIR) spectroscopy provides the information on the local environments of metal cations in the host material. The FTIR spectra of Ba_3La_2 $(BO_3)_4$: xSm^{3+} (x = 0, 0.02, 0.04, 0.06, 0.08 and 0.1 mol) were recorded in the region of 400 to 4000 cm^{-1} were shown in the Fig. 2(a) and an enlarged view of spectrum for 0.02 mol Sm^{3+} is shown in Fig. 2(b).

FTIR analysis is helpful to describe the unique vibrational bands and structural groups of B—O—B and these would cover the spectral wave number range from 600 to 1500 cm^{-1} [14]. The spectral bands observed at 1227 cm^{-1} and 1435 cm^{-1} were assigned to asymmetric stretching vibrations of B—O bond of trigonal BO_3 units, the bands observed at 870 cm^{-1}, 964 cm^{-1}, and 1074 cm^{-1} were ascribed to B—O symmetric stretching vibrations of tetrahedral BO_4 units. The shorter region bands observed at 590 cm^{-1}, 616 cm^{-1} and 741 cm^{-1} are corresponding to B—O—B bending vibrations of borate network [15]. The bands at 428 cm^{-1} and 457 cm^{-1} arisen from the bonds in La—O occurred in the lattice structure may be expected [16]. The other bands which were observed in the range from 2300 cm^{-1} to 4000 cm^{-1} were also ascribed may be due to the hydrogen bonds in the OH group [17]. All the details of FTIR assignments were depicted in Table 2.

3.3. FESEM and EDX analysis

FESEM analysis provides topographical information of sample surface at high magnifications of 5×, 10×, 100×, 1000×, etc. with virtual depth of field. For better clarity and high brightness of the photo shots, FESEM analysis of this phosphor powder was equipped with gold sputtering. In Fig. 3(i), (ii), (iii) and (iv), the surface morphology pictures of synthesized phosphor $Ba_3La_{1.9}(BO_3)_4$: 0.1 mol Sm^{3+} were captured and observed that the particles are submicron-sized, agglomerated and irregularly distributed over the surface. Since the micron level sizes of the particles, these phosphors can be good applications in solid-state lighting devices [18].

EDX is an analytical technique useful for the elemental analysis or chemical characterization of a sample. The EDX spectra of Ba_3La_2 $(BO_3)_4$: 0.1 mol Sm^{3+} sample was shown in Fig. 4 in which barium, lanthanum, oxygen, boron and samarium are presented. In addition, the weight% and atomic% of the starting elements in the synthesized material were also estimated from EDX data and the same were calculated theoretically which was shown in Table 3, found to have a good coincidence.

3.4. TG-DT analysis

Thermo gravimetric (TG) analysis is an analytical technique is used to determine the material's thermal stability also for the materials characterization through analysis of decomposition patterns. Where as in the differential thermal analysis (DTA) technique, the investigating sample is monitored with respect to a reference sample; both were heated at constant rate of temperature and measures the temperature difference between the sample and the reference so that exothermic and endothermic heat reactions may be detected.

As shown in the Fig. 5, both TG and DTA curves were depicted simultaneously as the sample Ba_3La_2 $(BO_3)_4$ was subjected to heat from room temperature to 800 °C. From TG curve it was cleared that, as the heating temperature increases, the sample undergone three stages decomposition and lost weight 1.813 % up to 80 °C, 4.192 % up to 462 °C and 1.263 % up to 763 °C. Later it was attained a stable state. A weight loss of 7.273 % was occurred and 92.727 % of its total weight was thermally stable. From the DTA curve, initially endothermic peaks up to 279 °C were may be ascribed to evaporation of water molecules and carbon dioxide molecules. An exothermic and endothermic occurred at 465 °C and 602 °C may be corresponding to the phase formation of $Ba_3La_2(BO_3)_4$ crystal.

Table 1
Crystalline size (D) and dislocation density (δ) of Sm^{3+} doped Ba_3La_2 $(BO_3)_4$ phosphor.

S.No.	Sm^{3+} ion (mol)	FWHM β (rad)	Diffraction angle (2θ)	$D = 0.89\lambda/\beta\cos\theta$ (nm)	$\delta = 1/D^2$ (nm^{-2})
1	$Sm^{3+} = 0$	0.00646	28.02°	22.14	0.00204
2	$Sm^{3+} = 0.02$	0.00496	28.13°	28.81	0.0012
3	$Sm^{3+} = 0.04$	0.00616	28.72°	23.25	0.00185
4	$Sm^{3+} = 0.06$	0.00564	27.87°	25.34	0.00155
5	$Sm^{3+} = 0.08$	0.00614	28.41°	23.29	0.00184
6	$Sm^{3+} = 0.1$	0.00648	28.63°	22.07	0.00205

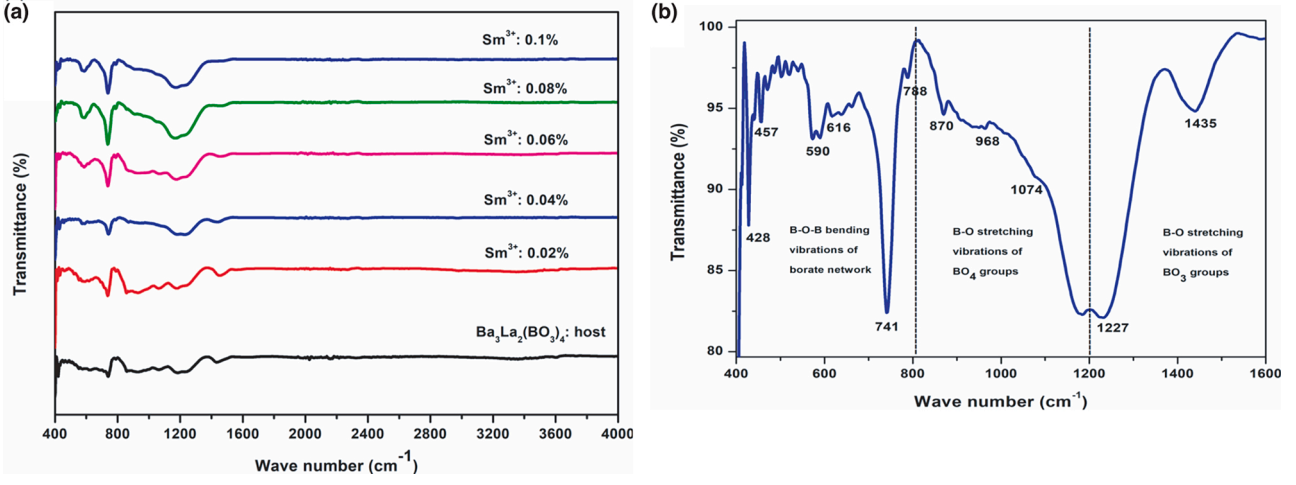

Fig. 2. (a). FTIR spectra band assignments of $Ba_3La_2(BO_3)_4$: Sm^{3+} and Fig. 2 (b). Bands enlarged view for 0.02 mol Sm^{3+}.

Table 2
FTIR bonding assignment details of $Ba_3La_2(BO_3)_4$: Sm^{3+}.

S.No.	Wave number (cm^{-1})	Bond assignment range	Type of bond assignment
1	1227 and 1435	1200–1600	B—O asymmetric stretching vibrations of trigonal BO_3 units
2	870, 964 and 1074	800–1200	B—O symmetric stretching vibrations of tetrahedral BO_4 units
3	590, 616 and 741	600–800	B—O—B bending vibrations of borate network
4	428 and 457	<600	La—O band lattice vibrations

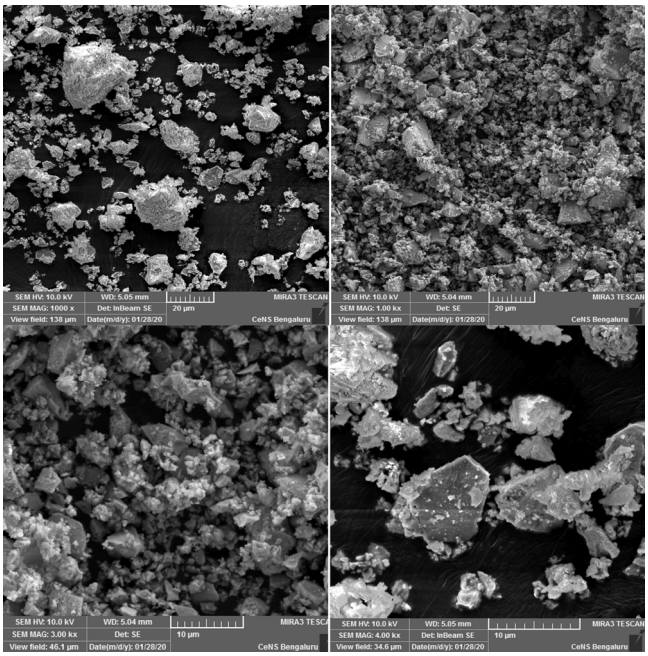

Fig. 3. FESEM images of phosphor materials with different resolutions.

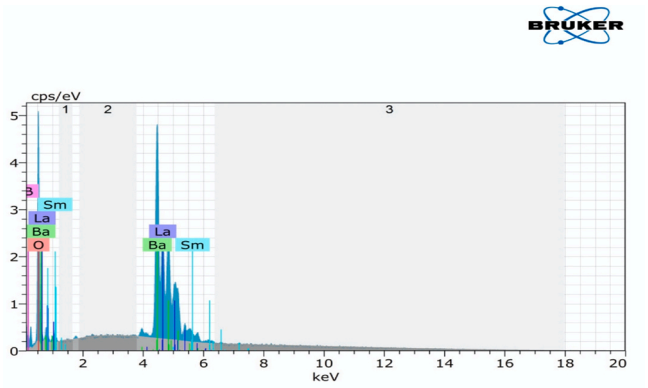

Spectrum: 1.txt

Element	Series	unn. C [wt.%]	norm. C [wt.%]	Atom. C [at.%]	Error (3 Sigma) [wt.%]
Oxygen	K-series	17.20	17.41	51.20	6.37
Barium	L-series	48.32	48.93	16.76	4.06
Lanthanum	L-series	25.45	25.78	8.73	2.17
Samarium	L-series	2.68	2.72	0.85	0.33
Boron	K-series	5.10	5.16	22.46	3.14
	Total:	98.75	100.00	100.00	

Fig. 4. EDX spectra analysis of Ba_3La_2 $(BO_3)_4$: 0.1 mol Sm^{3+}.

Table 3
EDX analysis showed weight percentages of starting elements in $Ba_3La_2(BO_3)_4$: 0.1 mol Sm^{3+}.

S.No.	Element	Atomic mass (units	Molecular weight	Weight% (calculated)	R = weight%/Atomic wt	Atomic% R/E
1	12 Oxygen	15.999	191.988	20.42	1.276	56.91
2	3 Barium	137.327	411.981	43.82	0.319	14.22
3	2 Lanthanum	138.905	277.81	29.55	0.212	9.45
4	0.1 Samarium	150.36	15.036	1.6	0.01	0.45
5	4 Boron	10.811	43.244	4.6	0.425	18.96
			Total: 940.06	99.99 %	2.242 (E)	99.99 %

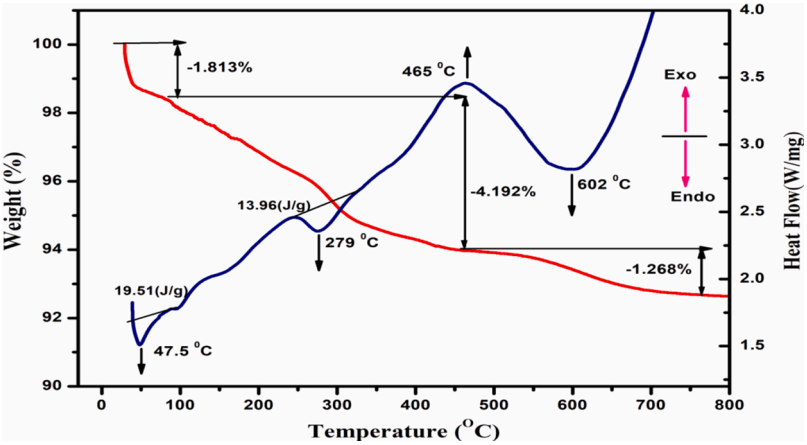

Fig. 5. Thermal study of phosphor sample carried by TGA and DTA.

3.5. DRS studies and band gap (E_g)

The diffuse reflectance spectrum (DRS) of $Ba_3La_2(BO_3)_4$ host sample is shown in the Fig. 6 in which a strong absorption band was observed in the wavelength region of 280−400 nm which can be due to electron passage from a valence band to conduction band. There was no weak absorption peaks observed in the region of UV–vis, which suggests that the surface defects, traps, impurities are very less [19].

The band gap of Ba_3La_2 $(BO_3)_4$ host materials can be calculated by using Kubelka-Munk function [20] using DRS spectra is

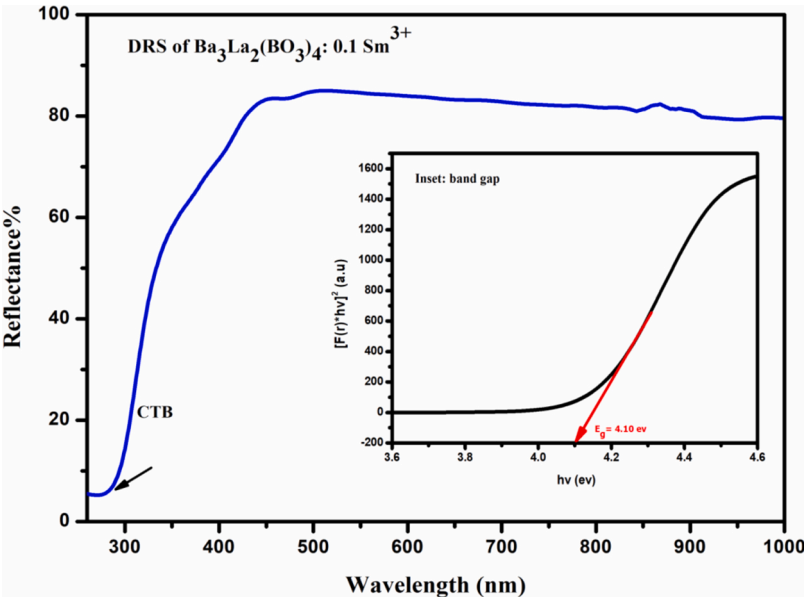

Fig. 6. DRS spectrum of Ba_3La_2 $(BO_3)_4$ and Tauc plot curve for energy band gap (inset).

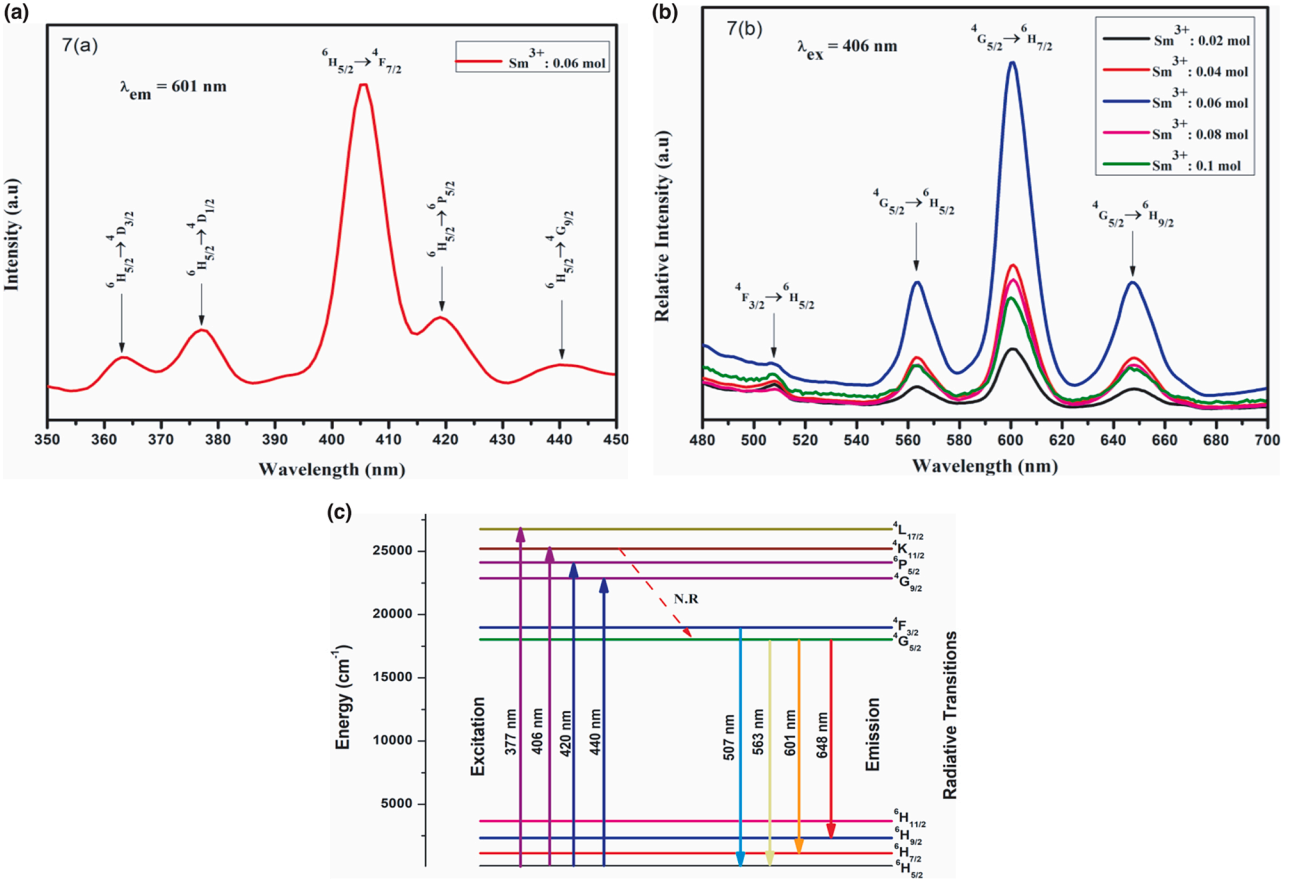

Fig. 7. (a) Excitation spectrum and 7 (b). Emission spectra of $Ba_3La_{2-x}(BO_3)_4$: Sm^{3+} phosphors. 7 (c). Empirical energy transitions diagram of Sm^{3+} in $Ba_3La_2(BO_3)_4$ phosphor.

$$F(R) = \frac{(1-R)^2}{2R} = \frac{K}{S} \quad (2)$$

where R is the diffuse reflectance percentage, K is the absorption coefficient and S be the scattering factor.

The linear absorption coefficient (α) and optical band gap (E_g) of a material, by Tauc relation is given by [21]

$$\alpha h\nu = C(h\nu - E_g)^n \quad (3)$$

Here hν is the energy of photon, C is the proportional constant called band tailing parameter and the exponent n is the power factor (n = 2)

The Eq. (3) is modified by using above Eq. (2) as

$$[F(R)h\nu]^2 = C(h\nu - E_g) \quad (4)$$

Now we plotted a graph with hν values on x-axis and $[F(R)h\nu]^2$ values on y-axis from which the extrapolation of linear fitted region intersected on x-axis can gives approximate band gap energy (E_g) of this sample. The inset graph in Fig. 6 have shown the band gap of $Ba_3La_2(BO_3)_4$ was estimated nearly 4.15 ev.

3.6. Photoluminescence studies

The emission and excitation spectra of $Ba_3La_{2-x}(BO_3)_4$: Sm^{3+} phosphors were recorded and shown in the Fig. 7(a). For the excitation spectrum, the sample was monitored at 601 nm and it consists of five excitation bands. The excitation bands were identified and assigned to respective transitions of Sm^{3+} ion, such as $^6H_{5/2} \rightarrow {}^4D_{3/2}$ at 365 nm, $^6H_{5/2} \rightarrow {}^4D_{1/2}$ at 377 nm, $^6H_{5/2} \rightarrow {}^4F_{7/2}$ at 406 nm, $^6H_{5/2} \rightarrow {}^6P_{5/2}$ at 420 nm and $^6H_{5/2} \rightarrow {}^4G_{9/2}$ at 440 nm [22]. All these bands were excitation transitions from ground state to higher energy states of Sm^{3+} ion. Among all these transitions, the band $^6H_{5/2} \rightarrow {}^4F_{7/2}$ at 406 nm has the highest excitation intensity and hence the emission spectra of phosphors were monitored under the excitation wavelength of 406 nm.

The photoluminescence emission spectra of $Ba_3La_2(BO_3)_4$: xSm^{3+} (x = 0.02, 0.04, 0.06, 0.08 and 0.1 mol) were recorded in the range of 450−700 nm. Fig. 7(b) shows the emission spectra phosphor samples monitored at an excitation wavelength 406 nm. The identified emission bands were raised due to the intra 4f transitions of Sm^{3+} ion, which were ascribed to $^4F_{3/2} \rightarrow {}^6H_{5/2}$ at 507 nm, $^4G_{5/2} \rightarrow {}^6H_{5/2}$ at 563 nm, $^4G_{5/2} \rightarrow {}^6H_{7/2}$ at 601 nm and $^4G_{5/2} \rightarrow {}^6H_{9/2}$ at 648 nm [23]. Among these emissions, the transition corresponding to $^4G_{5/2} \rightarrow {}^6H_{7/2}$ has the strongest emission intensity at 601 nm. This transition satisfied the selection rule of $\Delta J = \pm 1$, where J is the angular momentum. Magnetic dipole transitions obey the selection rule of $\Delta J = 0$ and ±1, and electric dipole transitions obey the selection rule of $\Delta J \leq 6$ unless J or $J' = 0$ when $\Delta J = 2, 3, 6$ [24]. The transitions $^4G_{5/2} \rightarrow {}^6H_{5/2}$ and $^4G_{5/2} \rightarrow {}^6H_{7/2}$ are magnetic dipole transitions, while the transition $^4G_{5/2} \rightarrow {}^6H_{9/2}$ is an electric dipole transition [25]. Also observed the emission intensity was raised and optimum for 0.06 mol concentration, further the intensity was decreased, obviously due to the concentration quenching effect. The 4f-4f partial energy transitions of Sm^{3+} ion were shown in the Fig. 7(c).

3.7. CIE color chromaticity

The performance and quality of emission color of the synthesized phosphor would dependent on the color coordinates lying in the CIE 1931 color chromaticity diagram. The coordinates for the optimum concentration of Sm^{3+} ion in $Ba_3La_2(BO_3)_4$ were calculated and reported as x = 0.5263 and y = 0.4519, and all the coordinates for other concentrations also be very close to these values as shown in Table 4. It was observed that these values were lying in the orange-red emission region as shown in the Fig. 8 of CIE diagram and hence this phosphor candidate may be useful for the application of orange-red emission color by pumped at NUV wavelength.

4. Conclusion

A new host material $Ba_3La_2(BO_3)_4$ in which various concentrations of Sm^{3+} ion doped phosphor samples were successfully synthesized by solid state reaction method and an orthorhombic crystal structure was confirmed. Thermal, structural, morphological characteristics have been studied by TG-DTA, XRD, FTIR, DRS and FESEM, EDX characterization techniques and properties were reported. From the PL spectra we have observed four emission peaks in which prominent emission intensity peak at 601 nm. The optimum concentration of Sm^{3+} is 0.06 mol for highest emission intensity and the color coordinates have been calculated as x = 0.5363 and y = 0.4519 which confirmed the emission color is lying in the orange-red region of the CIE 1931 diagram. From the characterization results such as, thermal stability, submicrons sized grains and perform optimum luminescence emission, this phosphor can be a good material for an orange-red light emission which might be applicable in solid-state lighting and LED display devices.

Funding

This research did not receive any specific grant from funding agencies in the public, commercial, or not-for-profit sectors.

Table 4
CIE color coordinates of Ba_3La_2 $(BO_3)_4$: Sm^{3+} phosphor.

S. No.	Sm^{3+} concentration (mol)	CIE coordinates	
		x	y
1	0.02	0.5241	0.4603
2	0.04	0.5363	0.4519
3	0.06	0.5007	0.4794
4	0.08	0.4908	0.4861
5	0.1	0.5257	0.4597

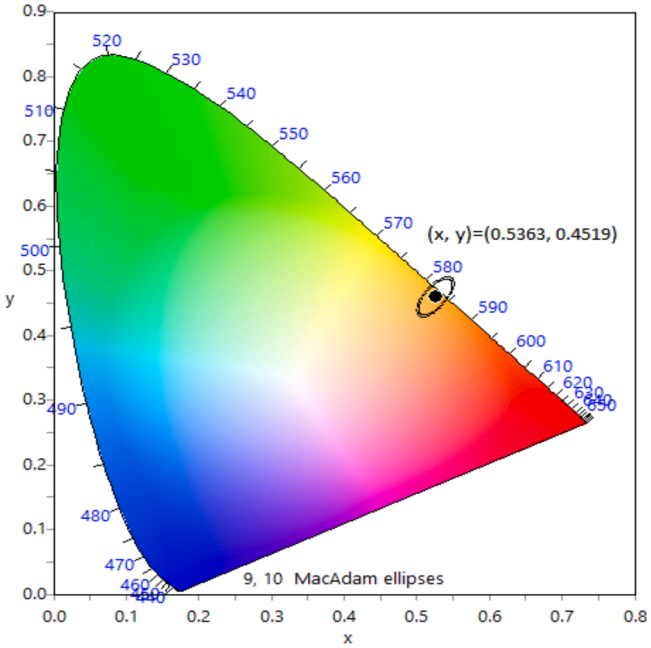

Fig. 8. CIE chromaticity diagram of Ba_3La_2 $(BO_3)_4$: 0.06 mol Sm^{3+} phosphor.

Declaration of Competing Interest

The authors report no declarations of interest.

References

[1] F.B. Xiong, H.F. Lin, X.G. Meng, H.X. Shen, W.Z. Zhu, Photoluminescence properties of a novel red emitting Pr3+- doped borate phosphor, Optik 159 (2018) 102–107.
[2] Bunala Chinna Jamalaiah, Shaik Nayab Rasool, Fluorescence properties of Sm3+ ions in yttrium aluminum borate phosphors for optical applications, J. Mol. Struct. 1097 (2015) 161–165.
[3] E.F. Schubert, J.K. Kim, Solid state light sources getting smart, Science 308 (5726) (2005) 1274–1278.
[4] H.A. Hoppe, Recent developments in the field of inorganic phosphors, Angew. Chem. Int. Ed. 48 (20) (2009) 3572–3582.
[5] C.C. Lin, R.S. Liu, Advances in phosphors for light-emitting diodes, J. Phys. Chem. Lett. 2 (11) (2011) 1268–1277.
[6] Hung-Rung Shih, Yee-Shin Chang, Structure and photoluminescence properties of Sm3+ Ion-Doped YInGe2O7 phosphor, Materials 10 (2017) 779, https://doi.org/10.3390/ma10070779.
[7] C.K. Lin, M. Yu, M.L. Pong, J. Lin, Photoluminescence properties of sol-gel derived (La, Gd) MgB5O10: Ce3+/Tb3+nano crystalline thin film, Opt. Mater. 28 (2006) 913–918.
[8] A.N. Yerpude, S.J. Dhoble, Luminescence properties of Eu2+ and Dy3+ ions in Ba4Al2O7 phosphor for solid state lighting, J. Lumin. 132 (2012) 1781–1785.
[9] K.N. Shinde, S.J. dhoble, Luminescence in Dy3+ and Eu3+activated K3Al2(PO4)3, J. Fluoresc. 21 (2011) 2053–2056.
[10] N.S. Bajaj, S.K. Omanwar, Combustion synthesis and characterization of phosphorKSr4(BO3)3: Dy3+, Opt. Mater. 35 (2013) 1222–1225.
[11] I. Koseva, P. Tzvetkov, P. Ivanov, A. Yordanova, V. Nikolov, Some investigatons on Tb3+ and Eu3+ doped Na2SiO3 as a material for LED application, Optik 168 (2018) 376–383.
[12] Fen Xiao, Rongxi Yi, Huiling Yuan, Guanjian Zang, Chengning Xie, Color tunable emission and energy transfer of Ce3+/Dy3+ codoped Ba3La2(BO3)4 phosphor for UV white LEDs, Spectrochim. Acta A. Mol. Biomol. Spectrosc. 202 (2018) 352–358.
[13] Vijaysingh, N. Singh, M.S. Pathak, Pramod K. Singh, V. Natarajan, Tb3+ doped Ca2La8(SiO4)6O2oxyapatite phosphors, Optik- Int. J. Light Electron Opt. 171 (2018) 356–362.
[14] C. Goutam, A.K. Yadav, A.K. Singh, ISRN Ceram, 1970, https://doi.org/10.5402/2012/428497.
[15] O. Annalakshmi, M.T. Jose, B. Venkatraman, G. Amarendra, Synthesis and study on the luminescence properties of cadmium borate phosphors, Mater. Res. Bull. 50 (2014) 494–498.

[16] Andrzej Machock, Theophilos Ioannides, Beata Stasinska, Wojciech Gac, George Avgouropoulos, Dimitris Delimaris, Wieslaw Grzegorczyk, Sylwia Pasieczna, Manganese-lanthanum oxides modified with silver for the catalytic combustion of methane, J. Catal. 227 (2004) 282–296.
[17] Parvinder Kaur, Simranpreet Kaur, Gurinder Pal Singh, D.P. Singh, Sm3+ doped lithium aluminoborate glasses for orange coloured visible laser host material, Solid State Commun. 171 (2013) 22–25.
[18] J.T. Ingle, A.B. Gawande, R.P. Sonekar, S.K. Omanwar, Yuhua Wang, Lei Zhao, J. Alloys Compd. 585 (2014) 633–636.
[19] Neharika, Vinay Kumar J. Sharma, Vivek K. Singh, O.M. Ntwaeaborwa, H.C. Swart, Surface and spectral studies of green emitting Sr3B2O6: Tb3+phosphor, J. Electron Spectros. Relat. Phenomena (2021), https://doi.org/10.1016/j.elspec.2015.11.011.
[20] P. Gupta, A.K. Bedyal, V. Kumar, Y. Khajuria, E. Coetsee-Hugo, O.M. Ntwaeaborwa, H.C. Swart, Opt. Mater. 36 (2014) 996–1001.
[21] J. Tauc, A. Menth, J. Non. Solids 8 (1972) 569–585.
[22] W.T. Carnall, H. Crosswhite, H.M. Crosswhite, Argonne Report ANL-78-95, 1978.
[23] Ranganathan Satheesh Kumar, Velladurai Ponnusamy, Phase formation and photoluminescence properties of Sm3+ doped Al5BO9 phosphor, Optik 126 (2015) 1224–1227.
[24] Z. Cui, R. Ye, D. Deng, Y. Hua, S. Zhao, G. Jia, C. Li, S. Xu, Eu2+/Sm3+ ions co-doped white light luminescence SrSiO3 glass-ceramics phosphor for white LED, J. Alloys. Compd. 509 (2011) 3553–3558.
[25] Myoung Gyu Ha, Jae-Sun Jeong, Kyoung-Rim Han, Yangsoo Kim, Ho-soon Yang, Euh Duck Jeong, K.S. Hong, Characterization and optical properties of Sm3+ -doped Sr2SiO4 phosphors, Ceramic Int. 38 (2012) 5521–5526.